Structure and mechanical properties of poly(butylene terephthalate)/rubber blends prepared by dynamic vulcanization

Masami Okamoto and Kiyoshi Shiomi
Toyobo Research Center, Toyobo Co. Ltd, Katata Ohtsu Shiga, 520-02, Japan

and Takashi Inoue*
Department of Organic and Polymeric Materials, Tokyo Institute of Technology, Ookayama, Meguro-ku, Tokyo, 152 Japan
(Received 2 December 1993; revised 1 April 1994)

We carried out the dynamic vulcanization of poly(butylene terephthalate) (PBT) with ethylene rubber having an epoxy group and investigated the morphology–mechanical properties relationship. The curing agent for the rubber used was adipic acid (AA). The AA-loaded (0.1 phr) 50/50 PBT/rubber blend had a two-phase structure of densely dispersed rubber particles in a PBT matrix and it showed excellent elastic behaviour, i.e. strain recovery after large deformation. To understand the elastic character, we constructed a two-dimensional model with five rubber inclusions in a PBT matrix and carried out an elastic–plastic analysis on the deformation mechanism by the finite-element method (FEM). FEM analysis revealed that, even in the highly deformed states in which almost the whole matrix has yielded due to the stress concentration, the ligament matrix between rubber inclusions in the stretching direction is preserved within the elastic limit to form an elastic field by interconnecting cured rubber particles. The tensile dilatometry test and transmission electron microscopy observation clearly showed internal cavitation of rubber particles. Insufficient strain recovery seems to be caused by the cavitation.

(Keywords: poly(butylene terephthalate); ethylene rubber; dynamic vulcanization)

INTRODUCTION

Dynamic vulcanization is a unique reactive processing that creases a two-phase structure with crosslinked particles of one polymer dispersed in a matrix of another. This reactive processing is providing a new class of thermoplastic elastomers[1]. In our previous paper, we discussed morphology development during dynamic vulcanization using light scattering[2]. In this paper, we extend the study of dynamic vulcanization to understand the morphology–mechanical properties relationship. The immiscible polymers employed are poly(butylene terephthalate) (PBT) and ethylene rubber with an epoxy group. The results are discussed with the aid of an elastic–plastic analysis on the deformation mechanism by the finite-element method (FEM).

EXPERIMENTAL

Materials

The PBT used in this study was a commercial product from Toyobo Co. ($M_n = 4.7 \times 10^4$; Toyobo Plastic Division). The rubber was a poly(ethylene-*co*-glycidyl methacrylate) copolymer, which was kindly supplied by Sumitomo Chemical Co. (Bondfast; methacrylate content = 3 mol%). The curing agent for the rubber used was adipic acid (AA), which reacts with the epoxy group. PBT, rubber and AA were melt-mixed in a co-rotating twin-screw extruder (Ikegai Machinery Corp.; 30 mm diameter, $L/D = 16$; barrel temperature = 250–260°C).

Flexural modulus and strain recovery tests

Flexural modulus was measured following the ASTM standard D-790 at a strain rate of 3 mm min^{-1}. Strain recovery was evaluated by a tensile set test: the tensile bar was stretched to a fixed certain strain (10–100%) at an elongation rate of 200% min^{-1}. The stretched specimen was held at this strain for 10 min and then released to shrink back. The tensile set value was calculated by:

$$\text{Tensile set } (\%) = (L_r - L_0)/(L_a - L_0) \quad (1)$$

where L_a is the gauge length at the applied strain, L_0 is the initial gauge length and L_r is the gauge length after the shrink back.

Uniaxial tensile dilatometry

Using the method of Bucknall[3], the tensile dilatometry experiment was carried out on a tensile testing machine under a constant axial strain rate of 200% min^{-1} using a standard ASTM D-638 specimen. The thickness strain

* To whom correspondence should be addressed

0032-3861/94/21/4618-05

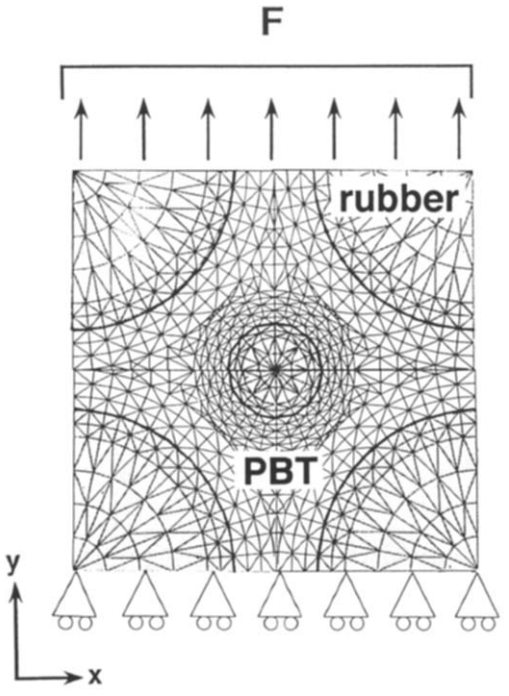

Figure 1 Two-dimensional FEM model with five rubber inclusions: PBT/rubber 50/50 model

was assumed to be the same as the width (transverse) strain ε_t. The volume strain, $\Delta V/V_0$, was calculated from:

$$\Delta V/V_0 = (1+\varepsilon_a)(1+\varepsilon_t)^2 - 1 \quad (2)$$

where ΔV is the volume change, V_0 is the original volume and ε_a is the axial strain.

Transmission electron microscopy

Injection-moulded specimens before and after the mechanical test were stained with RuO_4 vapour at room temperature for 20 h. The stained specimens were microtomed to an ultrathin section of 70 nm thickness using a Reichert–Jung ultracryomicrotome with a diamond knife at $-100°C$. The phase structure in the section was observed under an electron microscope, Hitachi H-600 (100 kV).

FEM analysis

To carry out the elastic–plastic analysis by FEM, it is necessary to know the true stress–true strain behaviour of the component polymers. Each polymer was injection moulded into a miniature rod-type dumbbell specimen by the Mini-Max Injection Molder (model CS-183; Custom Scientific Instruments Inc.) as described in the previous papers[4–6]. Tensile testing was carried out under a constant strain rate of 200% min^{-1} at room temperature. During stretching the diameter D of the specimen was observed by TV video camera. After the necking started, the diameter of thinned region was assumed to be D. From the time variation of D and the load P, true stress σ and true strain ε' were calculated:

$$\sigma = P/A = 4P/\pi D^2 \quad (3)$$

$$\varepsilon' = \ln \varepsilon = \ln(A_0/A) = 2\ln(D_0/D) \quad (4)$$

where A is the cross-sectional area of specimen and subscript 0 represents the unstretched state[7]. Thus a rod-type specimen is convenient to estimate the variation of A with stretching by watching just D.

We constructed a two-dimensional FEM model shown in *Figure 1*. Five rubber particles are embedded in a PBT matrix. This two-phase model is based on a TEM observation (see *Figure 2*). Volume ratio of PBT/rubber was set at 80/20 and 50/50. Each element was assumed to have mechanical properties identical to those of the

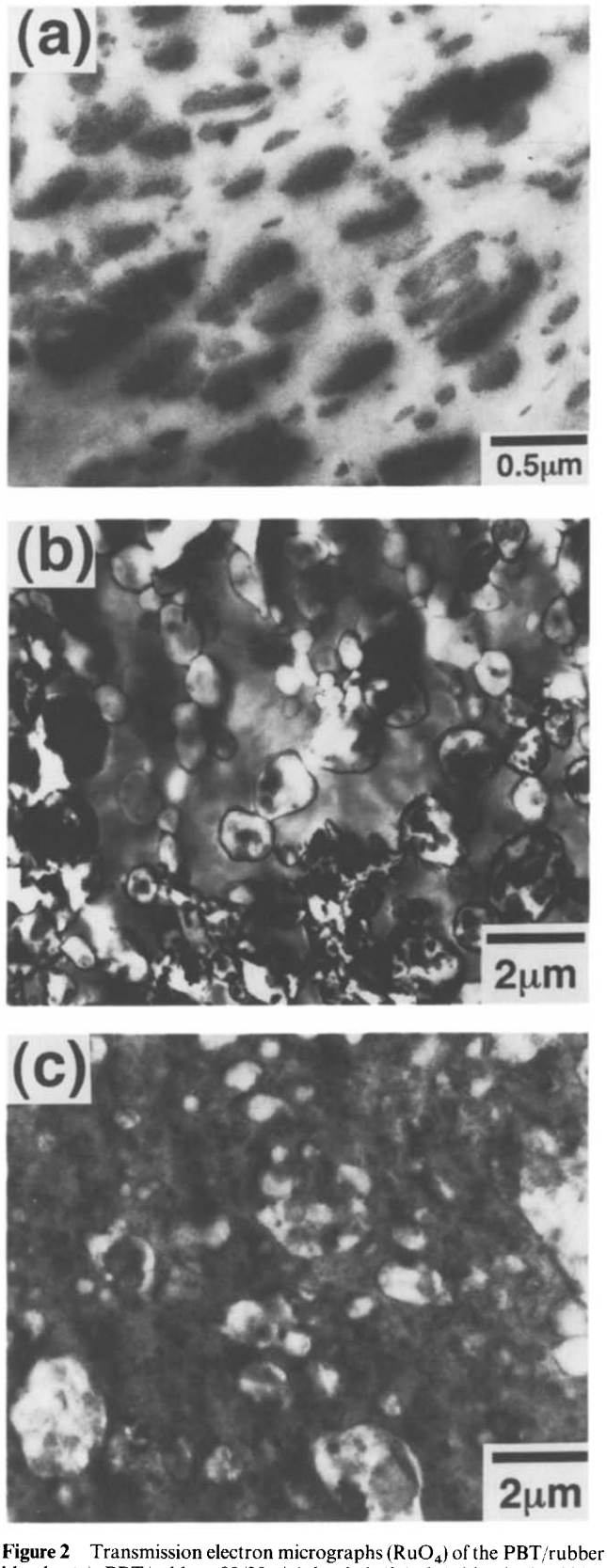

Figure 2 Transmission electron micrographs (RuO_4) of the PBT/rubber blends: (a) PBT/rubber 80/20 AA-loaded (0.1 phr) blend; (b) 50/50 AA-loaded (0.1 phr) blend; and (c) 50/50 AA-unloaded blend

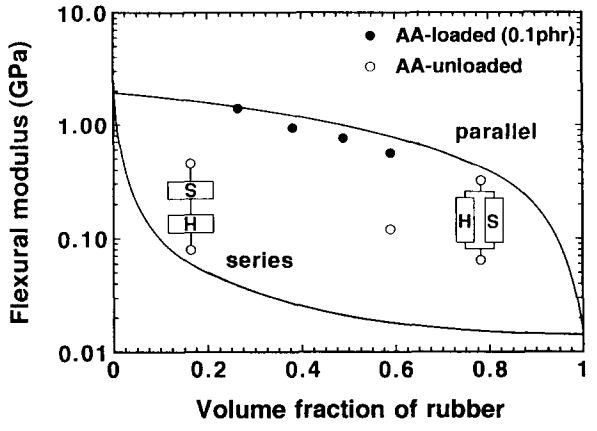

Figure 3 Variation of flexural modulus with volume fraction of rubber

neat component polymer. That is, it was assumed that the element exhibits the same true stress–true strain curve observed for the component polymer. Poisson's ratio of rubber was assumed to be 0.49 and that of PBT was 0.37.

The FEM model was uniaxially stretched in the y direction under the plane-strain condition ($\varepsilon_x = 0$). Stresses evolved in x, y and z directions, σ_x, σ_y, σ_z and shear stress τ_{xy} were calculated for each element as a function of bulk strain. Also calculated was the equivalent stress $\bar{\sigma}$ defined by:

$$\bar{\sigma} = \{\tfrac{1}{2}[(\sigma_x - \sigma_y)^2 + (\sigma_y - \sigma_z)^2 + (\sigma_z - \sigma_x)^2 + 6\tau_{xy}^2]\}^{1/2} \quad (5)$$

$\bar{\sigma}$ is assumed to be a reduced tensile stress, which is equivalent to the triaxial stress. The computer program used for FEM calculation was a two-dimensional non-linear version, EPIC-IV[8], which can deal with elastic–plastic mechanics. Numerical calculation was carried out on a large-scale computer (Sun-4 Work Station, Sun-Microsystem Inc.).

RESULTS AND DISCUSSION

Figure 2 shows the transmission electron micrographs of injection-moulded 80/20 and 50/50 PBT/rubber blends. In the 80/20 and 50/50 AA-loaded (0.1 phr) blend, one sees clearly dispersed rubber particles (dark phase regions in figure) in the continuous PBT phase (*Figures 2a* and *2b*); however, in the 50/50 AA-unloaded blend, large PBT particles (1–3 μm) are dispersed in the rubber matrix (*Figure 2c*). It suggests that, in the dynamic vulcanization process of 50/50 blend, phase inversion took place. This could be due to the viscosity increase of rubber phase with chain extension by AA. The fine dispersion of rubber in the PBT matrix may be due to the reaction between the epoxy group of rubber and the carboxylic acid end-group of PBT to yield an *in situ* formed PBT–rubber graft copolymer. After phase inversion, the graft copolymer suppresses the coagulation of rubber particles to render a fine dispersion[2].

In *Figure 3* is shown the flexural modulus as a function of rubber content. The two full curves are calculated by the series and parallel models. The parallel model has been successfully applied to describe the composition dependence of the modulus of two-phase material consisting of soft particles in a hard matrix. In contrast, the series model has been used for two-phase system of hard particles in a soft matrix[9]. The moduli of the blends prepared by dynamic vulcanization (full circles) are located on the parallel model line, suggesting the two-phase character of the hard component (PBT) matrix. In contrast, the modulus of the blend without AA (open circle) deviates very much from the line and it is rather close to the series model line. The results are consistent with the electron microscopic observation.

Figure 4 shows the strain recovery behaviour of the dynamically vulcanized blends. The tensile set increases with increasing applied strain. The set decreases on increasing the amount of crosslinked rubber, i.e. the dispersed rubber phase improves the elastic recovery of the blends. It was shown by FEM analysis that, even in the highly deformed states at which almost the whole matrix has been yielded by the stress concentration, the ligament matrix between rubber particles in the stretching direction is locally preserved within an elastic limit and acts as an *in situ* formed adhesive for connecting the rubber particles[4]. The larger the volume fraction of elastic region in the matrix, the higher overall elastic recovery is expected. Of course, in 50/50 and 80/20 blends in this paper, high level of elastic recovery cannot be expected since the volume fraction of rubber itself is low, compared with conventional thermoplastic elastomer[1]. However, it is interesting to investigate the deformation mechanism of such 50/50 and 80/20 blends.

Figure 5 shows the true stress–true strain (σ–ε') curves of PBT and AA cured rubber. The yield point was defined by a construction method, i.e. by drawing a tangent to the σ–ε' curve from a point on the ε' axis ($\sigma = 0$, $\varepsilon' = -1$). To simplify the FEM numerical calculation, the curve was approximated to be composed of two straight lines, as demonstrated by the broken lines for PBT in *Figure 5*.

In *Figure 6* are shown typical examples of the calculated results for deformed states during stretching (a–c) and recovery (d–f). Here the von Mises criterion for yielding had been applied for the FEM elements, i.e. the matrix elements yield when the equivalent stress $\bar{\sigma}$ from equation (5) exceeds the yield stress σ_y at the σ–ε' curve. The elements at which $\bar{\sigma}$ is larger than σ_y are shaded in *Figure 6*. One can see that the PBT matrix around rubber particles yields, as ε increases, and almost the whole matrix yields when ε attains 1.0. Note here that, even at $\varepsilon = 1.0$, the ligament matrix between rubber particles in the stretching direction still remains unshaded. It is locally preserved at low stress concentration ($\bar{\sigma} < \sigma_y$) within the elastic limit. The elastic matrix is expected to play the role of adhesive for connecting

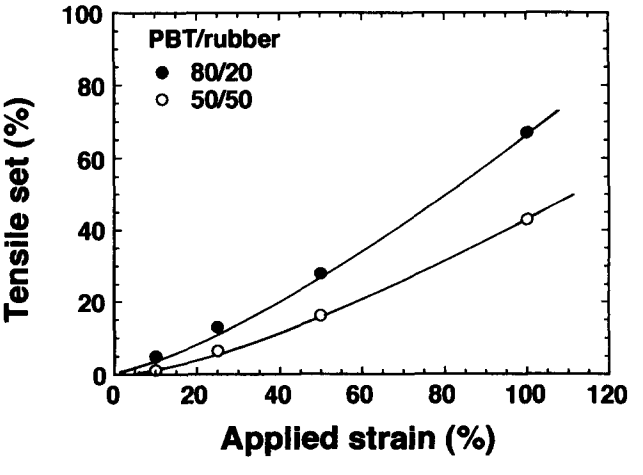

Figure 4 Strain recovery behaviour of PBT/rubber blend

rubber particles and provide a mechanism for the strain recovery of the two-phase system. One can also see the healing of strained triangles of matrix elements during the recovery process; the triangles (especially in shaded matrix) that are highly strained at high strains (*Figures 6c* and *6d*) can heal to those similar to original ones (compare *Figure 6f* with *Figure 6a* and *Figure 1*). The healing mechanism could be provided by the presence of rubber particles with high Poisson's ratio (≈ 0.5; no volume change with deformation.

Figure 7 shows the load (F)–strain curves simulated by FEM for the stretching and recovery process. The characteristic feature of the stress–strain of stretching and recovery behaviour is nicely described. The rubber content dependence of the residual strain is simulated fairly well. However, the observed values of residual strain (ca. 0.45 in *Figure 4*) are slightly larger than the calculated one (0.3 in *Figure 7*). The deviation could be associated with debonding at the rubber–matrix interface and void formation or cavitation in rubber particles. (Note that these effects are missed in the FEM analysis.)

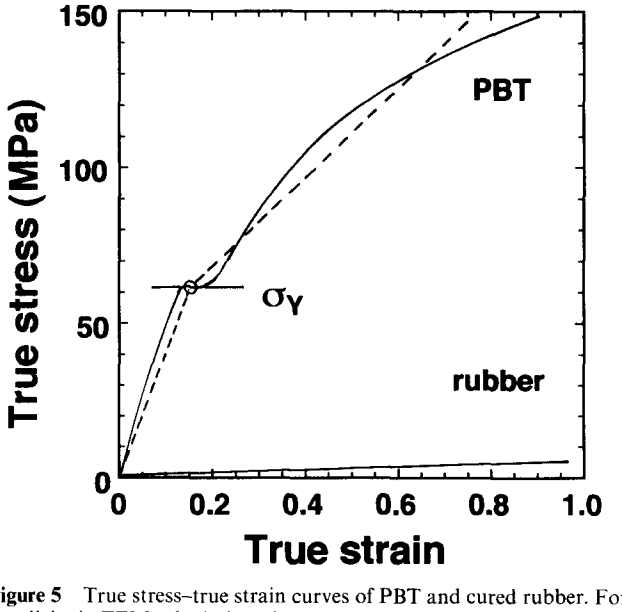

Figure 5 True stress–true strain curves of PBT and cured rubber. For simplicity in FEM calculation, the σ–ε' curve of PBT was approximated to be composed of two straight segments as indicated by broken lines

Figure 8 shows engineering stress–axial strain (σ–ε_a) and volume strain–axial strain ($\Delta V/V_0 - \varepsilon_a$) curves in the 50/50 blend. The initial volume increase could be entirely due to elastic deformation (Poisson's effect). At intermediate strains ($3\% < \varepsilon_a < 13\%$), the volume increase may be due to shear flow and void formation. The overall

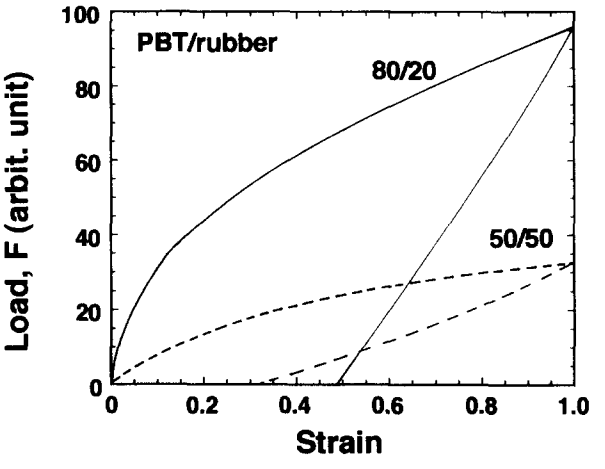

Figure 7 Load (F; see *Figure 1*) *versus* strain curves calculated by FEM for the stretching and recovery process

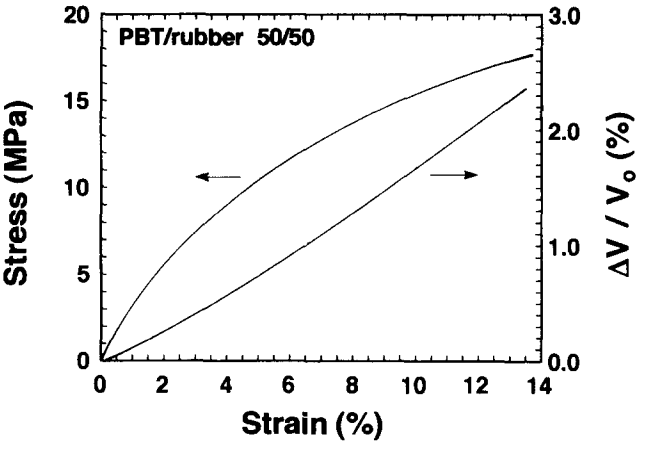

Figure 8 Stress–axial strain and volume strain–axial strain curves for the 50/50 PBt/rubber blend (0.1 phr AA-loaded)

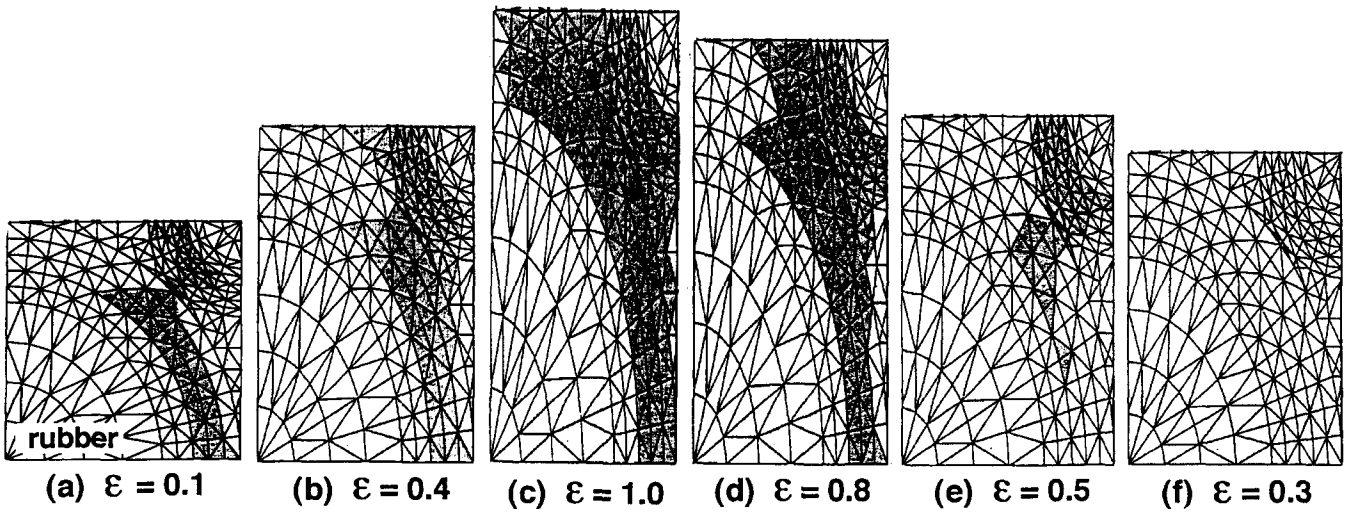

Figure 6 Deformation of FEM model: simulated results for the PBT/rubber 50/50 model of stretching (a–c) and of recovery (d–f). Yielded elements are shaded

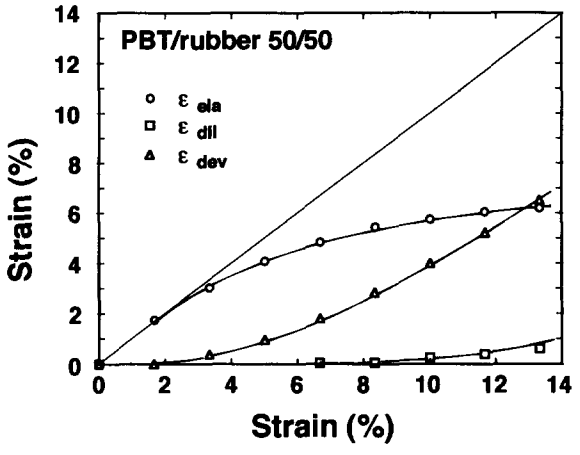

Figure 9 Elastic, deviatoric and dilational strains *versus* bulk strain for the 50/50 PBT/rubber blend (0.1 phr AA-loaded)

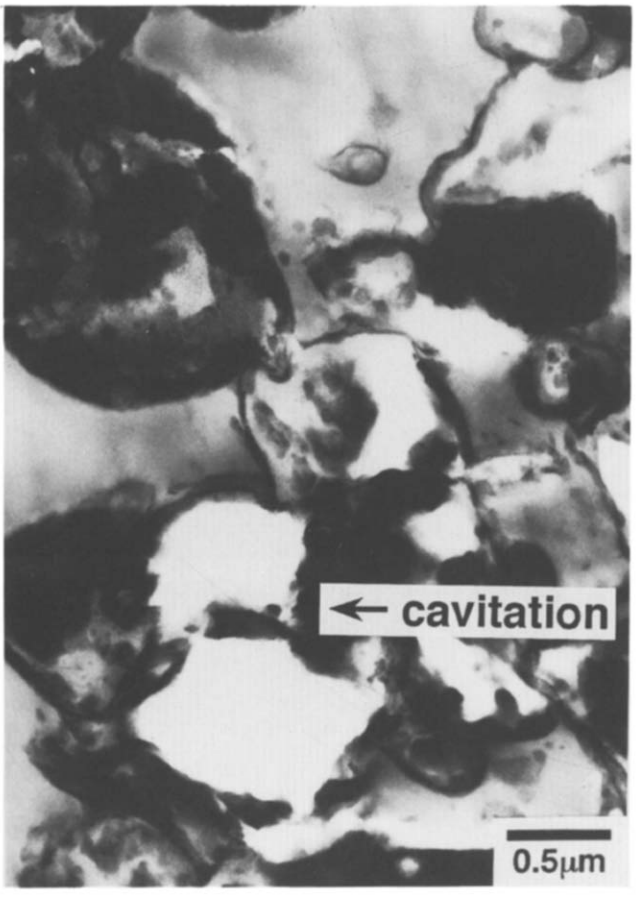

Figure 10 Transmission electron micrograph (RuO_4) of the 50/50 PBT/rubber blend (0.1 phr AA-loaded) after the strain recovery test ($\varepsilon = 1.0$). Arrow indicates cavitation in a rubber particles

volume strain can be divided into three contributions: the elastic ε_{ela}, the deviatoric (shear) ε_{dev} and the dilational (cavitation or void formation) ε_{dil}, assuming linear additivity[10]. The strain components are given by:

$$\varepsilon_{ela} = \sigma_y / E \tag{6}$$

$$\varepsilon_{dil} = \Delta V / V_0 - (1 - 2\nu)\sigma_y / E \tag{7}$$

$$\varepsilon_{dev} = \varepsilon - \Delta V / V_0 - 2\nu\sigma_y / E \tag{8}$$

where ν is Poisson's ratio, E is Young's modulus and σ_y is the yield stress. The calculated results are shown in *Figure 9*. One sees that there are definitely deviatoric and dilational contributions. The former starts to increase gradually when the latter appears. Anyhow, *Figure 8* suggests that void formation or cavitation could occur at fairly low strain.

The transmission electron micrograph of a specimen after the strain recovery test ($\varepsilon = 1.0$) is shown in *Figure 10*. As expected from the tensile dilatometry, one can see the cavitation of rubber particles. Thus, internal cavitation may result in insufficient strain recovery.

CONCLUSIONS

The crosslinked rubber particles could be densely dispersed in the PBT matrix by the dynamic vulcanization process. The 50/50 PBT/rubber blend showed excellent strain recovery. The elastic–plastic analysis by the two-dimensional FEM showed that, even in the highly deformed states, the ligament matrix between rubber inclusions in the stretching direction is locally preserved within an elastic limit (in the case of high rubber content) to provide strain recovery mechanism of the two-phase material. It was shown that strain recovery is deteriorated by cavitation in rubber particles.

REFERENCES

1 Coran, A. Y. 'Handbook of Elastomers—New Developments and Technology' (Eds A. K. Bhomwick and H. L. Stephens), Marcel Dekker, New York, 1988
2 Okamoto, M. and Inoue, T. *Kobunshi Ronbunshu* 1991, **48**, 657
3 Bucknall, C. B. 'Toughened Plastics', Applied Science, London, 1977
4 Kikuchi, Y., Fukui, T., Okada, T. and Inoue, T. *Polym. Eng. Sci.* 1991, **31**, 1029
5 Fukui, T., Kokuchi, Y. and Inoue, T. *Polymer* 1991, **32**, 2367
6 Kikuchi, Y., Fukui, T., Okada, T. and Inoue, T. *J. Appl. Polym. Sci., Appl. Polym. Symp.* 1992, **50**, 261
7 G'Shell, C. and Jonas, J. J. *J. Mater. Sci.* 1981, **16**, 1956
8 Yamada, Y. and Yokouchi, Y. 'Program EPIC IV for Elastic–Plastic Analysis by FEM', Baifukan, Tokyo, 1981
9 Takayanagi, M., Uemura, S. and Minami, S. *J. Polym. Sci. (C)* 1964, **5**, 113
10 Heikens, D., Sjoerdsma, S. D. and Coumans, W. J. *J. Mater. Sci.* 1981, **16**, 429